Electronic Supplementary Material (ESI) for Physical Chemistry Chemical Physics.

Supplementary Information for Lower degree of dissociation of pyruvic acid at water surface than in bulk

D. Lesnicki,[†] V. Wank,[‡,‖] J. Cyran,[¶] E. H. G. Backus,[*,‡,‖] and M. Sulpizi[*,§]

[†]*Institute of Physics, Johannes Gutenberg University Mainz, Staudingerweg 7, 55099 Mainz, Germany; Current address: Sorbonne Université, CNRS, Physico-Chimie des électrolytes et Nanosystèmes Interfaciaux, F-75005 Paris, France*

[‡]*University of Vienna, Faculty of Chemistry, Department of Physical Chemistry, Währinger Straße 42, 1090 Vienna, Austria.*

[¶]*Department of Chemistry and Biochemistry, Baylor University, 76706 Waco, Texas, USA*

[§]*Institute of Physics, Johannes Gutenberg University Mainz, Staudingerweg 7, 55099 Mainz, Germany; Current address: Department of Physics, Ruhr Universität Bochum, 44780 Bochum, Germany*

[‖]*University of Vienna, Vienna Doctoral School in Chemistry (DoSChem), Währinger Straße 42, 1090 Vienna, Austria*

E-mail: ellen.backus@univie.ac.at; sulpizi@uni-mainz.de;Marialore.Sulpizi@ruhr-uni-bochum.de

Experimental methods

Sample preparation: Pyruvic acid (PA 98 %, Sigma Aldrich) was purified by fractional vacuum distillation at reduced pressure. The pH values of PA were chosen based on the dissociation of the carboxylic acid group given by its pK_a. To set the different pH-values, NaOD (Sodium deuteroxide 40wt.% in D_2O, 99,5 atom % D, Sigma Aldrich) was added.

The samples were stored in sealed glass vials under dark conditions in the fridge (8°C) to avoid photo reactivity and dimerization.[1] The stability of the acid over a month was confirmed by NMR (Bruker Optik GmbH), ATR and VSFG. The VSFG and the ATR measurements were performed in solutions of D_2O instead of H_2O in order to avoid overlap of the ν_{AS,COO^-} and ν_{COOD} bands with the water bending mode located at ~ 1670 cm^{-1}.
The calibration of the used pH-Meter was performed with H_2O-solutions and therefore the measured pH value pH^* of the D_2O Samples were transformed to the pD-value. The calculation was carried out according to Krezel et al. and Gross-Butler-Purlee Theory with following equations[2] :

$$pD = pH^* + 0.44 \tag{1}$$

and

$$pH = 0.929 \times pD. \tag{2}$$

To measure the bulk and the air/liquid interface, ATR and VSFG spectroscopy were used.

ATR spectroscopy setup: For this study a Platinum FT-IR Tensor II with an ATR-Diamant-Unit from Bruker (Platinum ATR, Diamant-crystal) was used to measure PA in bulk. The angle of incidence of the IR beam was set at 45°. Measurements were 32 scans long and the spectral resolution was 4 cm^{-1} with an aperture of 6 mm. As a background measurement, D_2O was used and the data were analyzed with Opus software.

VSFG spectroscopy setup: The experimental setup was based on a femtosecond laser system with a 1 kHz Ti:Sapphire regenerative amplifier (Spectra-Physics Spitfire Ace) seeded by

a Mai Tai Ti:sapphire oscillator (Spectra-Physics). The laser system generated a wavelength of 800 nm, a pulse duration of around 40 fs, repetition rate of 1 kHz and pulse energy of 5 mJ. With an optical parametric amplifier (TOPAS-C, light conversion, Spectra-Physics) and a collinear DFG stage, part of the 800 nm light was converted to broadband infrared (IR) pulses. For the measurements the IR pulses were centered at 6450 nm (1626 cm^{-1}) to probe the carbonyl stretch vibrations. Another part of the light was spectrally narrowed by using a Fabry-Perot etalon (SLS Optik Ltd., bandwidth 15 cm^{-1}). Both beams were spatially and temporally overlapped on the sample to generate the SFG light. More details of the SFG-setup have been already reported.[3] For the data analysis, an additional background measurement was taken before each sample measurement. Thereby, the IR pulse was blocked and the visible light pulse was detected. At the end the background was subtracted from the spectrum and the spectrum subsequently divided by an VSFG spectrum from z-cut quartz.

The prepared PA solutions were pipetted directly into a round Teflon trough (8 cm diameters with a volume of 20 ml) and measured directly under N_2 atmosphere. These conditions ensure that no water vapor disturbs the beam path and thus the measurements. The VSFG spectra were acquired for 2 x 20 min and each sample was prepared and measured at room temperature 21 °C. All VSFG experiments were performed in duplicate and were acquired in ssp polarization combination (s-polarized VSFG, s-polarized VIS, and p-polarized IR).

Fitting: The ATR spectra were fitted with five Lorentzian functions in the frequency region from 1500 to 1800 cm^{-1} with constant central frequencies and widths of each Lorentzian peak. Although ATR spectra are often fitted with Gaussians, we choose Lorentzians to be consistent with the fits of the VSFG spectra commonly fitted with Lorentzian lineshapes. Table 1 presents the obtained parameters of each Lorentzian band. The VSFG data were

fitted with a combination of a NR signal and three Lorentzian line shapes:

$$I_{\mathrm{VSFG}} \propto \left| A_{\mathrm{NR}} e^{i\varphi_{\mathrm{NR}}} + \sum_{i=1}^{3} \frac{A_i}{\omega - \omega_i + i\Gamma_i} \right|^2 \tag{3}$$

where A_{NR} and φ_{NR} are the nonresonant amplitude and phase. A_i is the amplitude centered at the center frequency ω_i and $2\Gamma_i$ as the full width at half maximum of the i-th resonance, respectively. Table 2 presents the obtained parameters of the VSFG spectra fits.

Table S1: Fitting parameters for the ATR spectra of pyruvic acid

	ω_0 (cm^{-1})	1590	1614	1710	1729	1767
	Γ (cm^{-1})	23	20	14	18	20
pH	offset $\times 10^3$			A		
5.8	-8.3 ± 1.0	50.49±1.22	60.80 ± 0.87	10.35±0.52	0.21 ± 0.80	3.39±0.80
4.4	-9.9 ± 0.9	34.93±1.07	66.50 ± 0.77	10.96±0.45	0.96 ± 0.69	6.61±0.69
3.6	-10.1 ± 0.9	18.05±1.11	73.63 ± 0.79	12.47±0.47	2.22 ± 0.72	8.08±0.72
3.1	-7.6 ± 0.9	11.87±1.05	68.72 ± 0.75	12.30±0.45	5.42 ± 0.68	7.29±0.58
2.7	-5.2 ± 0.7	8.36±0.92	57.07 ± 0.65	11.38±0.39	10.66 ± 0.60	5.51±0.59
2.5	-2.3 ± 0.6	6.06±0.79	47.25 ± 0.56	10.70±0.34	15.64 ± 0.52	3.94±0.52
2.0	3.0 ± 0.4	2.32±0.53	26.06 ± 0.38	8.96±0.23	24.87 ± 0.35	0.61±0.35
1.7	5.0 ± 0.3	1.00±0.41	11.64 ± 0.29	8.11±0.18	30.66 ± 0.27	0.00±0.27
1.2	6.6 ± 0.4	0.64±0.49	3.23 ± 0.35	7.87±0.21	34.29 ± 0.32	0.00±0.32

Table S2: Fitting parameters for the SFG spectra of pyruvic acid

	ω_0 (cm^{-1})	1620	1708.5	1740.5
	Γ (cm^{-1})	46	46	23
pH	$A_{\mathrm{NR}} \times 10^2$		φ_{R} = -0.13	
5.8	10.32 ± 0.05	-2.27 ± 0.03	0.67 ±0.04	-0.03 ± 0.03
4.4	10.29 ± 0.06	-2.40 ± 0.04	1.13 ± 0.04	0.01 ± 0.02
3.6	10.40 ± 0.07	-2.51 ± 0.04	1.51 ± 0.04	0.20 ± 0.02
3.1	10.70 ± 0.09	-2.41 ± 0.05	1.79 ± 0.04	0.58 ± 0.02
2.7	11.09 ± 0.08	-1.99 ± 0.05	1.72 ± 0.04	0.97 ± 0.02
2.5	11.56 ± 0.06	-1.30 ± 0.05	1.55 ± 0.03	1.11 ± 0.02
2.0	10.79 ± 0.06	-0.34 ± 0.04	1.19 ± 0.03	1.28 ± 0.02
1.7	12.29 ± 0.05	-0.06 ± 0.03	1.08 ± 0.03	1.50 ± 0.02
1.2	13.10 ± 0.06	-0.01 ± 0.06	1.04 ± 0.04	1.55 ± 0.02

As shown in S2 and Fig.2 from the main paper, the fitted amplitudes from the ATR and VSFG spectra were normalized to the maximum area.

The acid base equilibrium reaction,

$$\mathrm{AH(aq) + H_2O(l) \rightleftarrows A^-(aq) + H_3O^+(aq)} \tag{4}$$

is described in general terms by the Henderson-Hasselbalch equation:

$$\mathrm{pH = pK_a + \log\left(\frac{[A^-]}{[AH]}\right)} \tag{5}$$

This equation gives us:

$$\mathrm{[AH] = 1/(1 + 10^{pH-pK_a})} \tag{6}$$

and

$$\mathrm{[A^-] = 1 - 10^{pK_a}/(10^{pK_a} + 10^{pH})}. \tag{7}$$

Based on the Henderson-Hasselbalch fit function Eq. 6 for the protonated (COOD) and Eq. 7 for the deprotonated (COO^-) species, the pK_a value of the bulk can be determined very accurately. At the interface, the fit equations are used as an approximation for the pK_a. The measurements and sample preparation were performed twice and the second measured and analyzed data set of pyruvic acid is shown in Figure S1 and S2. As described in the main paper the charged deprotonated form of pyruvic acid at the interface is not favored. Thus, the pyruvic acid molecules partially leave the surface with increasing pH. This surface depletion is reflected in the VSFG intensity of the carbonyl band at 1708 cm^{-1}. As is clear from Fig. S3 (graphically representing the amplitudes reported in Table S1), the SFG intensity of this mode decreases significant above pH=3. The slight drop in the bulk curve (1710 cm^{-1}) at around pH 4, is probably due to oligomer formation at higher pH values. The increase in both the bulk and surface intensity of the carbonyl peaks at low pH originates from the pH induced shift of the keto-hydrated equilibrium known from literature[4] and schematically depicted in Fig. S4a. Based on the NMR study by Pocker et al,[4] reporting on the fraction of hydration, we plot in Fig. S4b the keto fraction by taking one minus the values reported

for the hydrated form.

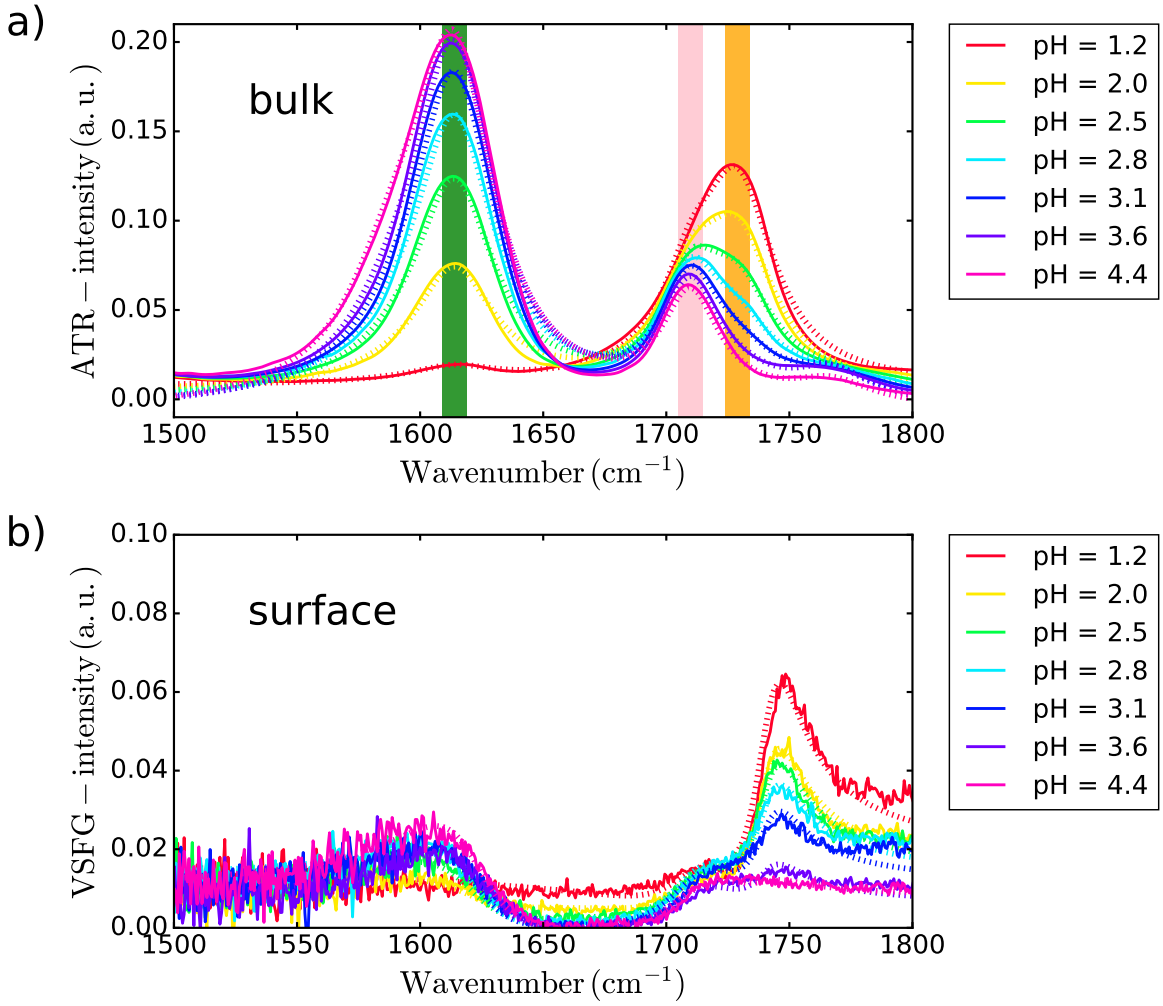

Figure S1: Second data set with the spectra in the frequency region of the carbonyl and carboxylate anion vibrations a) ATR and b) VSFG spectra at different pH values. The dashed lines represent the fits.

Simulations methods

To compute the difference in pK_a's between the aqueous value for the pyruvic acid and that at the water/air interface, we rely on the vertical energy gap method.[5] We use the scheme from our previous work[6] where the proton of the acid at the interface marked $(AH)_I$ is gradually transformed into a dummy $(Ad^-)_I$ (d is a particle with no charge) while the

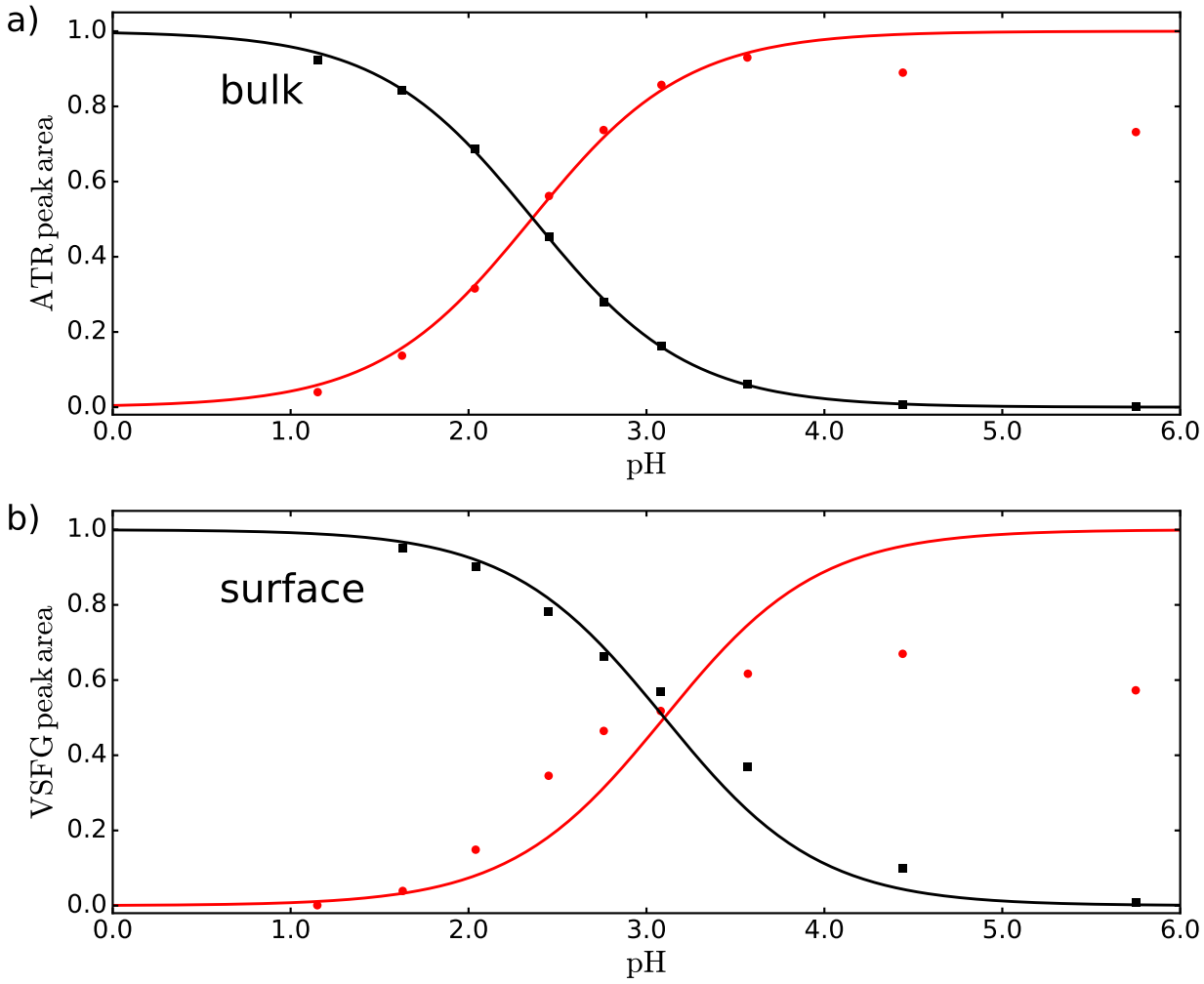

Figure S2: Second data set with normalized areas of the bands associated with the $\nu_{\mathrm{AS,COO^-}}$ (red, circles) and ν_{COOD} (black, squares) vibrations obtained from fitting a) ATR and b) VSFG spectra.

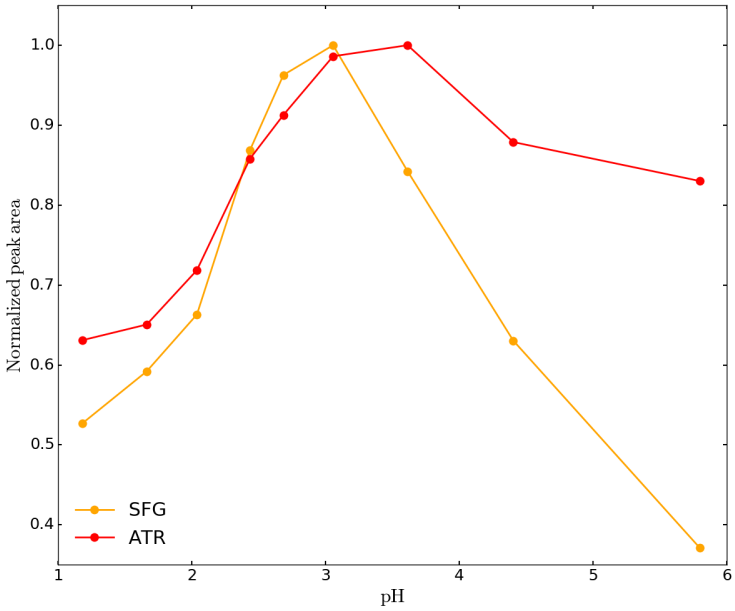

Figure S3: Normalized representation of the ATR fitting data (red) and SFG fitting data (orange) of the carbonyl band (C=O) of pyruvic acid as function of pH.

dummy atom in bulk water marked $(\mathrm{Ad}^-)_\mathrm{B}$ is gradually transformed into a proton $(\mathrm{AH})_\mathrm{B}$ as shown schematically in Fig. S5.

The free energy change of this process is calculated using the thermodynamic integration technique:

$$\Delta A = \int_0^1 d\eta \langle \Delta E \rangle_\eta \tag{8}$$

where $\Delta E = E_1 - E_0$ is the vertical energy gap, defined as the potential energy difference between product P: $\left((\mathrm{Ad}^-)_\mathrm{I}, (\mathrm{AH})_\mathrm{B}\right)$ and reactant R: $\left((\mathrm{AH})_\mathrm{I}, (\mathrm{Ad}^-)_\mathrm{B}\right)$ configurations extracted from the molecular dynamics trajectory. The subscript η indicates that the averages are evaluated over the restrained mapping Hamiltonian

$$\mathcal{H}_\eta = (1-\eta)\mathcal{H}_R + \eta\mathcal{H}_P + V_r \tag{9}$$

where η is a coupling parameter which gradually increased from 0 $\left((\mathrm{AH})_\mathrm{I}, (\mathrm{Ad}^-)_\mathrm{B}\right)$ to 1 $\left((\mathrm{Ad}^-)_\mathrm{I}, (\mathrm{AH})_\mathrm{B}\right)$ and $\mathcal{H}_R$ and $\mathcal{H}_P$ stand for the reactant and product states, respectively.

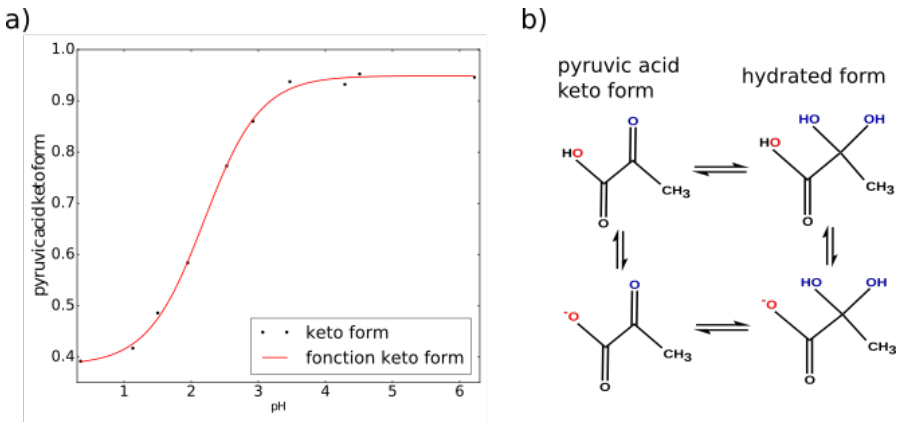

Figure S4: a) Fraction of molecules in the keto form for a 1.3 M pyruvic acid solution as a function of pH taken from literature.[4] b) Schematic illustration of the keto-hydrated equilibrium of pyruvic acid in solution

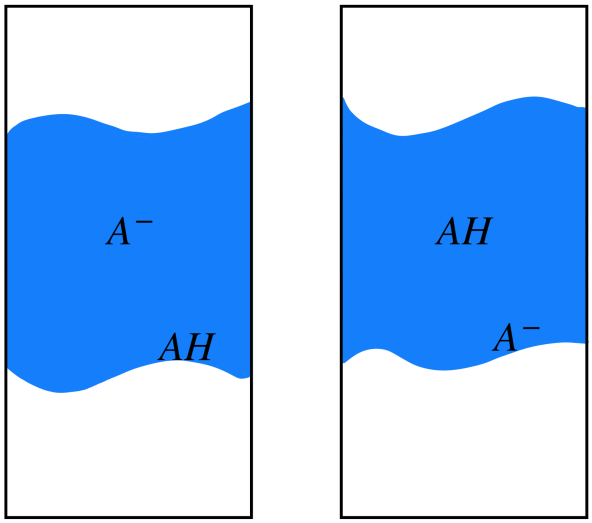

Figure S5: Schematic view of the simulation setup used for the calculation of ΔpK_a value: a) the initital state with protonated acid (AH) at the interface and deprotonated acid (A^-) in the bulk. b) the final state with the acid in the bulk (AH) and the deprotonated acid (A^-) at the interface.

The restrained harmonic potential V_r, which is used to keep the dummy position close to where it was in the protonated state,

$$V_r = \sum_{bonds} \frac{k_r}{2}(r - r_{eq})^2 + \sum_{angles} \frac{k_\theta}{2}(\theta - \theta_{eq})^2 + \sum_{dihedrals} \frac{k_\phi}{2}(\phi - \phi_{eq})^2 \tag{10}$$

consists of the bonding, angle bending and dihedrals torsion terms whose equilibrium values are r_{eq}, θ_{eq}, ϕ_{eq} respectively.

As we are interested to compare the acidity of the pyruvic acid at the interface to the bulk, we start by identifying the free energy deprotonation of the pyruvic acid at the interface and in the bulk, respectively,

$$(\Delta_{dp} A_{AH})_I = \int_0^1 d\eta \, \langle (\Delta_{dp} E_{AH})_I \rangle_\eta \tag{11}$$

and

$$(\Delta_{dp}A_{AH})_B = \int_0^1 d\eta \, \langle (\Delta_{dp}E_{AH})_B \rangle_\eta \tag{12}$$

with $(\Delta_{dp}E_{AH})_I = E_{1I} - E_{0I}$ and $(\Delta_{dp}E_{AH})_B = E_{1B} - E_{0B}$. If we assume that the desolvation free energy of the aqueous proton, the translational entropy generated from the acid dissociation and the free energy for the quantum correction for the nuclear motion are similar in the bulk and at the interface, the difference in pK_a's is simply related to the deprotonation free energy for interface (I) and bulk (B), $(\Delta_{dp}A_{\mathrm{AH}})_{I,B}$ by

$$\Delta \mathrm{pK_a} = \mathrm{pK}_{a_I} - \mathrm{pK}_{a_B} = \frac{(\Delta_{dp}A_{\mathrm{AH}})_I - (\Delta_{dp}A_{\mathrm{AH}})_B}{ln10k_BT} \tag{13}$$

Using the thermodynamic integral Eq. 8 and the assumption that along the trajectory the two acids do not interact with each other, we can treat separately the deprotonation of the acid in the bulk (labeled B) and at the interface (labeled I): $E_1 - E_0 = (E_{1I} + E_{0B}) - (E_{0I} + E_{1B})$. As a consequence, we can write,

$$\Delta \mathrm{pK_a} = \frac{1}{ln10k_BT} \int_0^1 d\eta \langle \Delta E \rangle_{r\eta} \tag{14}$$

The final $\Delta \mathrm{pK_a}$ reads as

$$\Delta \mathrm{pK_a} = \frac{1}{6ln10k_BT}(\langle \Delta E \rangle_0 + \langle \Delta E \rangle_1) + \frac{2}{3ln10k_BT}\langle \Delta E \rangle_{0.5} \tag{15}$$

using the 3-point Simpson rule for the integral in Eq. 14

DFT based Born-Oppenheimer molecular dynamics (DFTMD) simulations were performed using Becke exchange[7] and Lee, Yang and Parr[8] correlation functionals. All calculations have been carried out with the freely available DFT package CP2K/Quickstep which is based on the hybrid Gaussian and plane wave method.[9] Analytic Goedecker-Tecter-Hutter pseudopotentials,[10,11] a TZV2P level basis set for the orbitals and a density cutoff of 280

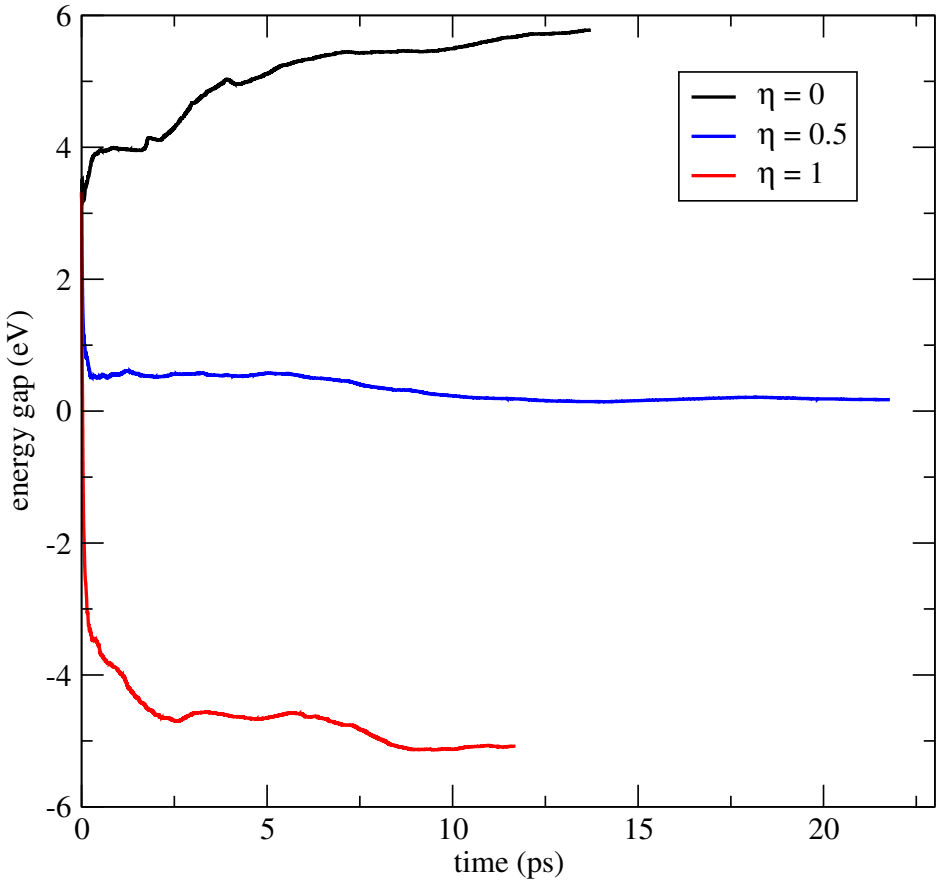

Figure S6: Accumulative averages of vertical energy gaps with $\eta = 0$, 0.5 and 1 as a function of time.

Ry were used. Dynamics were conducted in the canonical NVT ensemble with a timestep of 0.5 fs using the CSVR thermostat with the target temperature of 330 K to avoid the glassy behavior of BLYP water and a time constant of 1 ps. A periodic orthorhombic box of dimensions 19.64×17.008×60.0 Å is considered. For both bulk and interface the most stable *Tce* isomer was considered.[12] For the ΔpK_a calculation, trajectories of 9.8 ps for $\lambda = 0$ (acid deprotonated in bulk) and 11.75 ps for $\lambda = 1$ (acid deprotonated at the interface) were used.

Vertical Energy Gaps

Figure S6 shows the vertical energy gap for different values of η as a function of time. Using Eq. 15 we find that the interfacial pyruvic acid is less acidic than the one in the bulk by pK_a units of 3.9.

References

(1) Perkins, R. J.; Shoemaker, R. K.; Carpenter, B. K.; Vaida, V. Chemical Equilibria and Kinetics in Aqueous Solutions of Zymonic Acid. *J. Phys. Chem. A* **2016**, *120*, 10096–10107, PMID: 27991786.

(2) Krezel, A.; Bal, W. A formula for correlating pKa values determined in D2O and H2O. *J. Inorg. Biochem.* **2004**, *98*, 161–166.

(3) Dreier, L. B.; Nagata, Y.; Lutz, H.; Gonella, G.; Hunger, J.; Backus, E. H. G.; Bonn, M. Saturation of charge-induced water alignment at model membrane surfaces. *Sci. Adv.* **2018**, *4*, eaap7415.

(4) Pocker, Y.; Meany, J. E.; Nist, B. J.; Zadorojny, C. Reversible hydration of pyruvic acid. I. Equilibrium studies. *J. Phys. Chem.* **1969**, *73*, 2879–2882.

(5) Sulpizi, M.; Sprik, M. Acidity constants from vertical energy gaps: density functional theory based molecular dynamics implementation. *Phys. Chem. Chem. Phys.* **2008**, *10*, 5238–5249.

(6) Parashar, S.; Lesnicki, D.; Sulpizi, M. Increased Acid Dissociation at the Quartz/Water Interface. *J. Phys. Chem. Lett.* **2018**, *9*, 2186–2189.

(7) Becke, A. D. Density-functional exchange-energy approximation with correct asymptotic behavior. *Phys. Rev. A* **1988**, *38*, 3098–3100.

(8) Lee, C.; Yang, W.; Parr, R. G. Development of the Colle-Salvetti correlation-energy formula into a functional of the electron density. *Phys. Rev. B* **1988**, *37*, 785–789.

(9) VandeVondele, J.; Krack, M.; Mohamed, F.; Parrinello, M.; Chassaing, T.; Hutter, J. Quickstep: Fast and accurate density functional calculations using a mixed Gaussian and plane waves approach. *Comput. Phys. Commun.* **2005**, *167*, 103 – 128.

(10) Goedecker, S.; Teter, M.; Hutter, J. Separable dual-space Gaussian pseudopotentials. *Phys. Rev. B* **1996**, *54*, 1703–1710.

(11) Hartwigsen, C.; Goedecker, S.; Hutter, J. Relativistic separable dual-space Gaussian pseudopotentials from H to Rn. *Phys. Rev. B* **1998**, *58*, 3641–3662.

(12) Kakkar, R.; Pathak, M.; Radhika, N. P. A DFT study of the structures of pyruvic acid isomers and their decarboxylation. *Org. Biomol. Chem.* **2006**, *4*, 886–895.